

# Automatic ROI for Remote Photoplethysmography using PPG and Color Features

Elisa Calvo-Gallego<sup>1</sup> and Gerard de Haan<sup>2</sup>

<sup>1</sup>*Instituto de Microelectrónica de Sevilla (IMSE-CNM), CSIC-University of Sevilla, Seville, Spain*

<sup>2</sup>*Eindhoven University of Technology, Eindhoven, The Netherlands*

**Keywords:** Biomedical Monitoring, Photoplethysmography (PPG), Image Analysis, Skin Detection, Fuzzy Logic.

**Abstract:** Remote photoplethysmography (rPPG) enables contact-less monitoring of the blood volume pulse using a regular camera, thus providing valuable information about the cardiovascular system. However, the quality of the acquired rPPG signal is strongly affected by the region of skin where the analysis is carried out and, therefore, to be confident of obtaining valid information, a pre-selection of the region-of-interest (ROI) for the PPG analysis is necessary. In this paper, we propose a method for the automatic extraction of this ROI combining the local characteristics of the PPG-signal with the color information using fuzzy logic. Results of the quality of the ROI extraction and its application on pulse rate detection are provided.

## 1 INTRODUCTION

Photoplethysmography (PPG) is an optical technique that allows monitoring of vital signals, such as pulse or respiratory rate, from the optical absorption variations of the human skin caused by the blood volume variations during the cardiac cycle.

The first reference to this technique dates from 1930s (Hertzman, 1937), when the first characterizations of the PPG signals, the capture of the first recordings from human fingers and the first measures of blood volume changes from PPG signals in different situations, like exercise and exposure to cold of the subject, were carried out and published. At the time, the origin of the different components of the PPG signal were only partially understood. However, it was generally accepted that they could provide valuable information about the cardiovascular system and, consequently, research on this topic continued. It was not until 1980s when many of these advances gave rise to the creation of a commercial device, a pulse-oximeter, which greatly increased the relevance of these studies in clinical care (Allen, 2007).

Due to its low-cost and its non invasiveness, efforts to develop PPG have been multiplied recently, following mainly two lines of research. On one hand, the desire of preventing contact in extreme sensitivity cases (e.g. neonates, patients with burns) or situations requiring strict unobtrusiveness (e.g. surveillance, fitness) and the ambition of removing the sen-

sitivity to the varying force or pressure of the probe on the skin, has promoted the evolution towards remote PPG (rPPG) (Huelsbusch et al., 2002), (Takano et al., 2007). On the other hand, studies in ambient light conditions using regular video cameras have been done to replace dedicated light sources (typically red/infra-red wavelength), initially used as a result of a shallower penetration depth in skin (Verkruysse et al., 2008).

The quality of the acquired rPPG signal is strongly affected by the subject motion, the region and type of skin (defined mainly by its thickness and its color, in turn determined by the concentration of melanin in the epidermis and the concentration of hemoglobin in the dermal blood vessels) and the illumination.

Many studies have been aimed at increasing the robustness against motion and changing illumination conditions. This is where the use of an RGB-video camera is advantageous, as it simultaneously provides multiple color channels with different PPG and noise mixtures. To retrieve the desired clean signal from the observed set without prior information about the mixing process, Blind Source Separation (BSS) techniques have been used for decades in this kind of physiological measurement applications e.g. in multi-channel electroencephalogram and electrocardiogram (Glass, 2004). Indeed, motion robust methods to find the pulse-signal, i.e. the pulsatile component of the PPG, from video using BSS have been described in (Huelsbusch et al., 2002), (Poh et

al., 2010), or (Lewandowska et al., 2011). A different, chrominance-based, approach was used by (de Haan et al., 2013) who assumed non-local intensity-variation and specular reflection to cause the main distortions. Furthermore, they assumed a constant standardized skin-color, which enabled them to construct a linear combination of the normalized mean skin-color signals orthogonal to the assumed distortions regardless the color of the illumination. This eliminated the periodicity-based component-selection of BSS-based methods, which performed poorly on fitness videos with their strong periodic subject motion.

To segment the relevant skin regions for remote-PPG, however, not much progress has been documented. The majority of the publications need a segmentation of the ROI, either manually or, using a face detector which involves an increase of computational complexity, a limitation of the part of skin that can be detected, or the necessity of an initialization or periodic reset process (Lempe et al., 2013).

At this point, this paper aims to contribute by proposing an automatic ROI-detection in a video sequence for remote PPG analysis. This goal is achieved with a system (Fig. 1) that uses the output of the pursued application (the PPG analysis), combining it with other input (the color, specifically the hue component), to detect the pixels belonging to human skin (that is, the ROI). The idea is that, in a later processing stage, from this skin template, the performed PPG analysis or the conclusions obtained from it can be filtered, modified or/and improved and, to demonstrate it, a simple system for automatically obtaining the pulse rate of a person in a video sequence is presented. Since the inputs of the proposed system are already required by the application, the added computational complexity is low (barely some comparators and multipliers).

The reason to combine the different kinds of information is mainly to reinforce the classification process made by systems based on a single feature, owing to the fact that, as a result of the already mentioned problems to acquire a good PPG signal under certain scenarios and to similar circumstances with the color, decisions taken in those process could be wrong or undetermined. Due to that imprecise nature of data, fuzzy logic inference systems have been considered for the mixture. They are universal interpolators which allow to perform any non-linear mapping

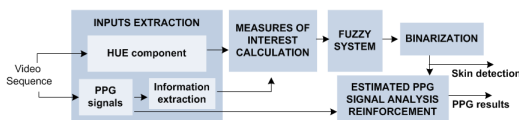


Figure 1: Block diagram of the proposed system.

between the input and output space.

The paper is organized as follows. In Sections II and III, the methods for the calculation of the inputs of the fuzzy system as well as the reasons for its choice are briefly explained. Section II is focused on rPPG signals and information obtained from them whereas Section III is centered on the acquisition of chromatic information of the image. Section IV describes the proposed fuzzy system for skin detection. This system is composed by two rule-bases whose functionality is to calculate the probability of belonging to a skin fuzzy set (first rule base) and to adjust dynamically the threshold for a final binarization process (skin/non-skin) (second rule base). Assessment details and simulations results are summarized in Section V and VI. The obtained conclusions are exposed in Section VII.

## 2 PPG PROCESSING

The first feature for skin-detection extracted from the video sequence is based on an analysis of PPG signals in the frequency domain.

PPG signals are obtained using the chrominance-based method of (de Haan et al., 2013) since this concept has demonstrated a relevant improvement on motion robustness against earlier proposed blind source separation techniques. Our system, illustrated in Fig. 2, adds a true-motion estimation block to achieve pixel alignment ((de Haan et al., 1994),(de Haan, 2010)). Later, a 2048 point Fast Fourier Transform (FFT) is applied on the Hanning windowed PPG signals and a peak detection and a signal-to-noise rate calculation are carried out in the signals.

The position of the maximum peak of the signal provides the pulse rate (P), that is, the rate of heart contractions, measured in beats/min. Since, for adults, this value lies between 30 beats/min (in case of a well trained athlete, in rest) and 240 beats/min (in case of a person at maximum level exercise), the peak detection is limited to that frequency interval.

The signal-to-noise rate (SNR) provides the relation between the energy around the fundamental frequency plus the first harmonic of the pulse signal and the remaining energy contained in the spectrum. It is computed using Eq. (1), where harmonics of the spectrum of the PPG signal (denoted as  $\hat{S}(f)$ ) are isolated using unitary templates around them ( $U_i(f)$ ).

$$SNR = 10 * \log_{10} \left( \frac{\sum_{30}^{240} (U_i(f) \hat{S}(f))^2}{\sum_{30}^{240} ((1 - U_i(f)) \hat{S}(f))^2} \right) \quad (1)$$

In Fig. 3.b, an example of a PPG signal in the frequency domain calculated in one pixel of the example

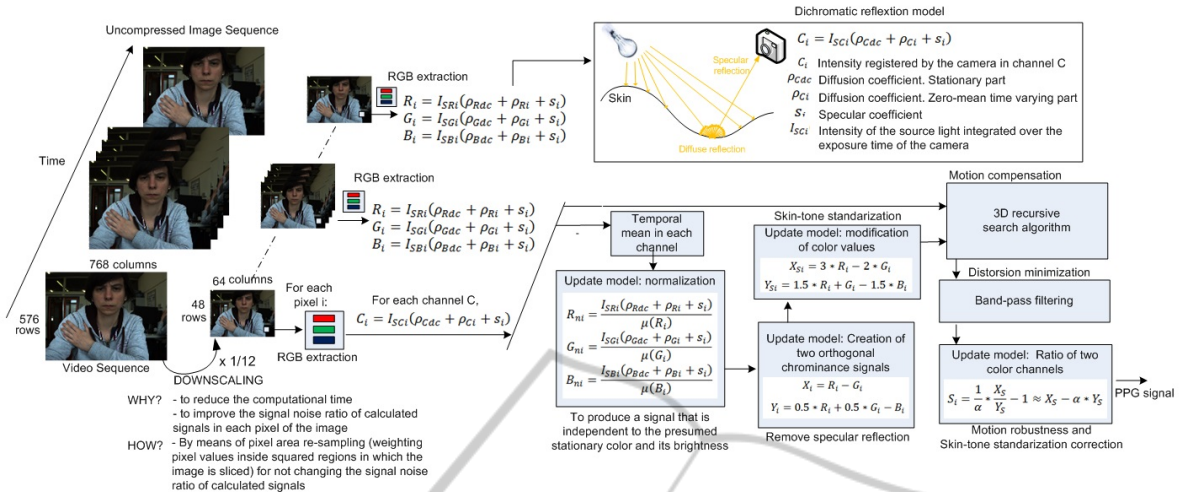


Figure 2: Flowchart of considered PPG signal extraction.

frame is shown. The values of detected P and SNR in the whole image are shown in 3.d and 3.e, where brighter pixels indicate higher values of these magnitudes. It can be recognized that skin pixels have a relatively high SNR (up to 10 dB) and a valid pulse rate value (in this case, 82 beats/min). In pixels where SNR and pulse rate values are not the expected, for example in the neck, it is considered that the PPG signal has not been acquired with sufficient quality.

The appreciable homogeneity of these magnitudes in the skin regions leads to the definition of other two measures as inputs of the system:

- **Uniformity of the pulse rate (HP):** A 3 x 3 window is considered around each pixel of P to calculate the number of pairs in that window in which differences between pulse rate values exceed a threshold (Eq. 2 and 3, being  $Th_p=5$ ). This allows us to measure the uniformity of P, checking how many pixels are substantially equal in the neighborhood. The values of this matrix are between 0 and 81. As shown in Fig. 3.d, pulse rate values are equal or homogeneous in skin regions. For that reason, HP matrix (Fig. 3.g) has higher values in skin areas than in non skin areas.

$$HP_{ij} = \sum_{v=j-1}^{j+1} \sum_{u=i-1}^{i+1} \sum_{s=j-1}^{j+1} \sum_{r=i-1}^{i+1} (d(u, r, v, s)) \quad (2)$$

$$d(u, r, v, s) = 1 \text{ if } \text{abs}(P(u, v) - P(r, s)) \geq Th_p \quad (3)$$

$$d(u, r, v, s) = 0 \text{ if } \text{otherwise}$$

The computational cost of this equation can be reduced removing (v,u) = (s,r) pairs and (r,u,s,v) combinations.

- **Uniformity of SNR (TSNR, values in natural units):** The texture of the SNR values in a 9 x 9 neighborhood centered in each pixel is calculated

by means of an entropy filter. It has been computed using the 'entropyfilt' instruction of Matlab whose theoretical base is Eq. (4), where  $p(u,v)$  is the probability of (u,v) value in the considered sub-histogram. TSNR values normally fall between 0 and 10, being lower when the texture of that SNR sub-matrix is less random, this means softer in changes. For that reason, values are higher in points where PPG signal is detected, i.e. in skin areas. An example of TSNR matrix is shown in Fig. 3.h.

$$TSNR_{ij} = \sum_{v=j-4}^{j+4} ( \sum_{u=i-4}^{i+4} (p(u,v) * \log_2(p(u,v))) ) \quad (4)$$

### 3 COLOR PROCESSING

The majority of methods proposed in the literature for skin detection are based on color, texture, or appearance features. In general, the major drawbacks of many textures and object detection methods like face-detectors are that they can not deal with different skin-regions, partial occlusion or changes in the object position or scale, moreover their computational complexity is high. Consequently, our search for features to complement the PPG-signal has focused on color methods that, in many situations, allow to overcome these kind of problems ((Kelly et al., 2008)-(Kakumanu et al., 2007)). One of the simplest possible options, a thresholding of the hue component of the image (Fig. 3.f), was initially selected as as measure of interest for the considered system. Later, to work with a more reliable measure, also an index of hue homogeneity was calculated as follows (Fig. 3.i):

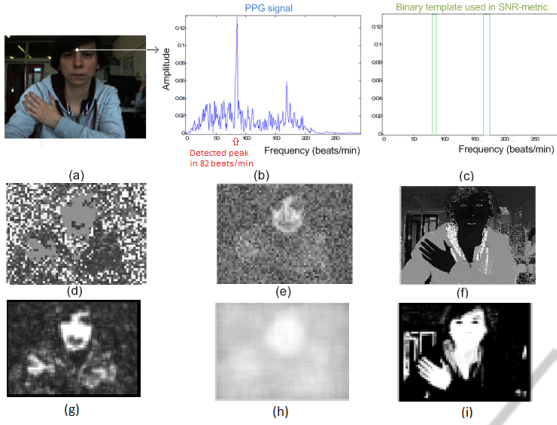


Figure 3: (a) Example frame, (b) PPG signal in frequency domain for a pixel belonging to forehead, (c) Binary template window for calculating SNR in case (b), (d) P, (e) SNR, (f) Hue component, (g) HP, (h) TSNR, (i) HI.

- Hue index (HI): In the whole image, the hue (H) and the uniformity of the hue (HH) in each pixel are evaluated. HH is calculated in the same way that it was previously done with pulse rate (Eq. 2). If both measures are in a specific range (Eq. 5, where  $Th_{hl} = 0.1$ ,  $Th_{hs} = 0.95$  and  $Th_{hh} = 60$ ) it is considered that this pixel belongs to skin and the  $HI_{nds}$  acquires '1' value in that pixel. Otherwise, a zero value is assigned to it. After that, a downscaling process is done over HI (Eq. 6, where  $n=12$ ) as it was done with the original image in Fig. 2. The values of this final matrix are between 0 and 1, being values closer to '1' when the probability of skin in that pixel is higher.

$$HI_{nds,ij} = [(H_{ij} < Th_{hl}) \vee (H_{ij} > Th_{hs})] \circ [HH_{ij} > Th_{hh}] \quad (5)$$

$$HI_{ds,ij} = \frac{1}{n^2} \sum_{v=(j-1)*n-1}^{j*n} \left( \sum_{u=(i-1)*n-1}^{i*n} HI_{nds}(u,v) \right) \quad (6)$$

## 4 FUZZY SYSTEM

The contribution presented in this paper is a hierarchical system composed by two rule-bases.

The first rule base combines, in each pixel, HP, HI, TSNR and SNR to provide a value in the interval [0,1] that indicates the probability of belonging of a pixel to the skin or, in other words, the membership grade to a skin fuzzy subset. While closer to '1', the belonging to skin will be higher. The set of IF-THEN rules that defines this subsystem is shown in Table 1. It has been deduced from the following principles, obtained analyzing the inputs of the system.

Table 1: Fuzzy skin detection rule base.

ID	IF	ANTECEDENTS	THEN	CONSEQ	
1	HI = LARGE	AND HP = LARGE		SKIN	
2	HI = LARGE	AND TSNR = LARGE		SKIN	
3	HI = SMALL	AND HP = LARGE	AND TSNR = LARGE	AND SNR = LARGE	SKIN
3	OTHERWISE			NON-SKIN	

- Normally, color information is more reliable than PPG information. However, it is insufficient for reliable classification.
- False positive cases in a classification process based only on HI matrix are mainly due to noisy dark areas and some red areas such as clothes or the mouth of the person. They can be reduced corroborating HI decision with some other inputs: HP or TSNR. If HI is large and, either HP or TSNR are large, the output should be skin. SNR is not used in these situations since it is very dependent on the the quality of the acquired signal.
- False negative cases in a classification process based only on HI matrix results occur, e.g. when there are highlights in the face of the person. They can be reduced if, in case HI was small, HP, TSNR and SNR are all large.

As this heuristic knowledge does not provide enough information to determine the values that define the fuzzy sets of the antecedents, a tuning process has been employed to adjust them, using the well-known supervised learning Marquardt-Levenberg algorithm within of the fuzzy system development environment Xfuzzy 3.3 (Xfuzzy WebPage). Typical values in the literature have been selected as initial value for the Hessian addition (0.2) and the increase/decrease adaptation factors (2 and 0.2, respectively). The training has been performed with some prepared files, composed by sets of inputs/output patterns generated for one or several video test sequences. The final considered fuzzy sets for each input variable are shown in Fig. 4. The fuzzy mean has been chosen as defuzzification method, generating the output of the system as the mean of the consequent values (defined by two singleton fuzzy sets in zero and one), weighted by its activation grade.

The second rule base allows to calculate dynamically the threshold used in the final binary classification into skin and non-skin sets. The inputs to this rule-base are three indexes that measure the quality of the types of information by means of the variance of its values in each frame, being it calculated according Eq. 7 and 8 ( $nc$  is the number of columns of the frame and  $nf$  is the number of rows of the frame). These inputs are represented using fuzzy sets whose membership grade are shown in Fig. 5.

$$V = \frac{1}{nc * nf} \sum_{v=1}^{nf} \left( \sum_{u=1}^{nc} (x_{uv} - \mu)^2 \right) \quad (7)$$

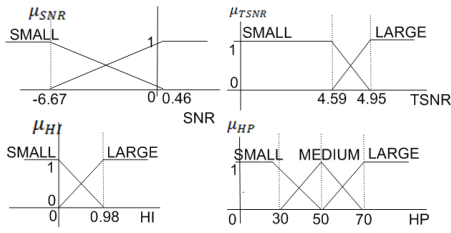


Figure 4: Fuzzy skin detection rule-base: Membership functions for the fuzzy sets.

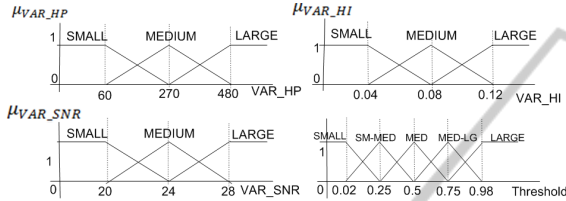


Figure 5: Fuzzy threshold calculation: Membership functions for the fuzzy sets.

$$\mu = \frac{1}{nc * nf} \sum_{v=1}^{nf} \left( \sum_{u=1}^{nc} x_{uv} \right) \quad (8)$$

In these sets, the variances of the SNR and HP values (VAR\_SNR and VAR\_HP, respectively) are small when few pixels have a high value of these magnitudes. This can be why, either skin regions are small or the quality of the acquired PPG signals is not good. VAR\_SNR and VAR\_HP are medium when, either the quality of the acquired PPG signals is medium or there are regions with very good quality and regions with very bad quality. And, finally, VAR\_SNR and VAR\_HP are large when the quality of the PPG input is usually good and region is medium in size. With the last input, the variance of the hue index values (VAR\_HI), the followed reasoning is similar. It is small when, in few pixels, there is a dominant color in the red range and as before, this can be why, either skin regions are small or the quality of hue component is not good. If VAR\_HI is medium, it can be considered that the quality of hue is good although it also happens that red areas have been detected in the image but not in the correct position. If VAR\_HI is large, either the skin areas are large or the number of red range false positive cases in the image is high.

Taking these ideas into account, in general, when the value of these three indexes are small, the output of the first rule base is less defined, that is, it is closer to zero. Then, threshold should be also small. If one or several indexes are high, the value of the threshold will increase, but when the three indexes are high, the subject in the image is usually taken the whole image up. In this case, it is necessary to decrease the value of the threshold. This knowledge has been expressed using the rule set shown in Table 2.

Table 2: Fuzzy threshold calculation for binarization.

ID	IF	ANTECEDENTS	THEN	CONSEQ
1	VAR_HI = SMALL	AND VAR_SNR = SMALL		SMALL
2	VAR_HI = SMALL	AND VAR_SNR = MEDIUM	AND VAR_HP = SMALL	SMALL
3	VAR_HI = SMALL	AND VAR_SNR = MEDIUM	AND VAR_HP = LARGE	MEDIUM
4	VAR_HI = SMALL	AND VAR_SNR = LARGE		MED-LG
5	VAR_HI = MEDIUM	AND VAR_SNR = SMALL	AND VAR_HP = SMALL	SM-MED
6	VAR_HI = MEDIUM	AND VAR_SNR = SMALL	AND VAR_HP = MEDIUM	MEDIUM
7	VAR_HI = MEDIUM	AND VAR_SNR = MEDIUM		MEDIUM
8	VAR_HI = MEDIUM	AND VAR_SNR = LARGE		MEDIUM
9	VAR_HI = LARGE	AND VAR_SNR = SMALL	AND VAR_HP = SMALL	SM-MED
10	VAR_HI = LARGE	AND VAR_SNR = MEDIUM	AND VAR_HP = SMALL	MEDIUM
11	VAR_HI = LARGE	AND VAR_SNR = MEDIUM	AND VAR_HP = MEDIUM	MEDIUM
12	VAR_HI = LARGE	AND VAR_SNR = MEDIUM	AND VAR_HP = LARGE	MED-LG
13	VAR_HI = LARGE	AND VAR_SNR = LARGE	AND VAR_HP = MEDIUM	LARGE
14	VAR_HI = LARGE	AND VAR_SNR = LARGE	AND VAR_HP = LARGE	MEDIUM

The output variable has been defined by means of five fuzzy sets which has been also shown in Fig.5. As in the first subsystem, the fuzzy mean algorithm has been used as defuzzification method.

## 5 SETUP AND VIDEO DATABASE

A 768 x 576 pixels, 8-bit, global shutter RGB CCD camera (type USB UI-2230SE-C of IDS GmbH) with a flexible C-mount lens (Tamron 12VM412ASIR), operated at 20 frames/s, has been used for recording some videos to test the system. The duration of the video recording was set to 2 min and uncompressed data were stored. Subjects were asked to sit and relax for 2 min prior to the recording to ensure a stable pulse rate. Also, they were asked to remain stationary for the duration of the recordings.

A total of 22 video sequences with 18 people with different skin-types have been used in the final tests. The followed nomenclature for identifying the mentioned recordings is: L1-L2N, where L1 is I, II, III, IV or V (roughly estimated skin-type on Fitzpatrick scale), L2 is M, or F (Male, or Female subject), and N is the number of recordings of this type that have been captured. Following this terminology, V-M1 means the first sequence registering a male subject having an estimated skin-type V on Fitzpatrick's scale.

## 6 SIMULATIONS RESULTS

Fig. 6 shows some examples of sequences that have been processed. The first seven rows describe the behavior of the first rule-base. Examining them, it is possible to extract mainly three conclusions:

- Both, PPG information and hue information, play an important role in the system. In I-M1 and I-F1 video sequences, for example, it is the PPG input which provide more confident information since a bad hue index detection has been done as a result

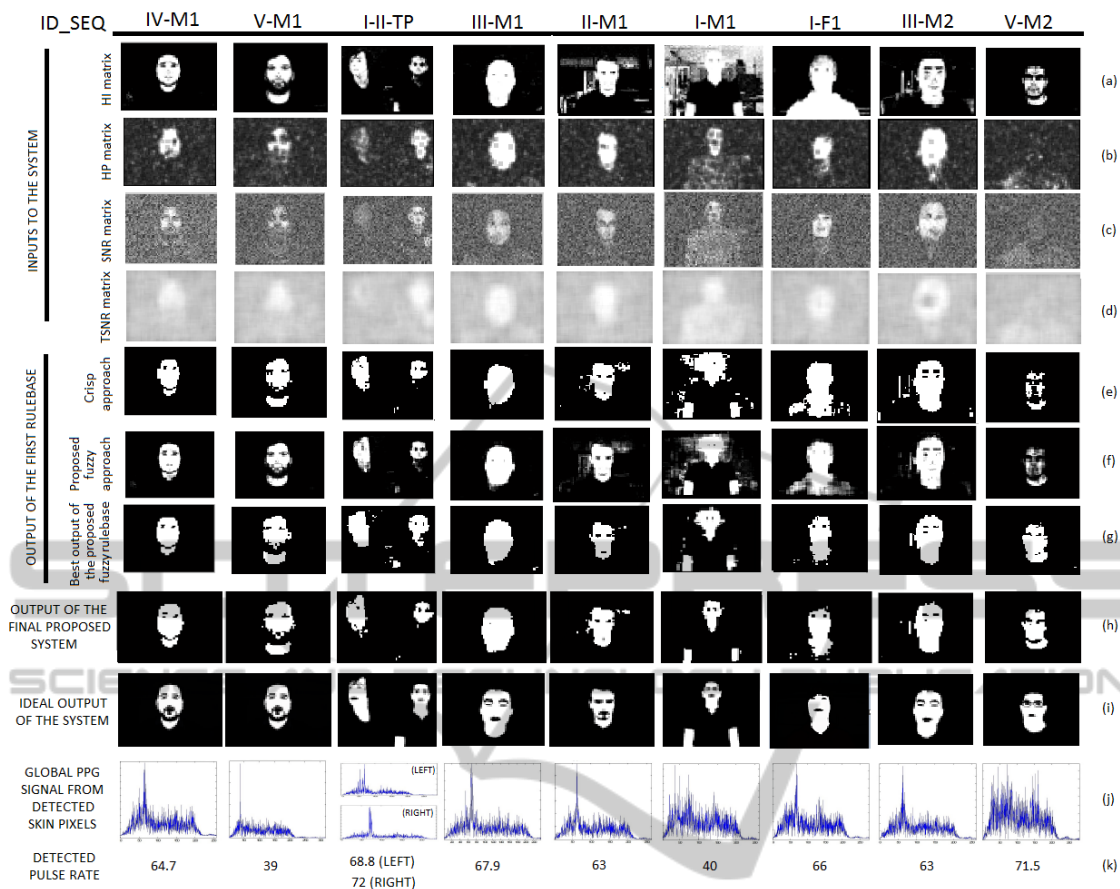


Figure 6: (a)-(d) Inputs of the first rule-base, (e) Output of the crisp approach for the first rule-base (f) Fuzzy output of the first rulebase (g) Best output of the first rule-base calculated by means of the true and the false success rate trade-off in the performed classification (See ROC Curves (Oberti et al., 1999)) (h) Output of the proposed final system (i) Ideal hand-segmented output of the skin detection system (j) Global PPG signal in the image (k) Detected pulse rate from (j).

of red colors clothes and noise. In other cases, however, such as V-M2, magnitudes obtained from PPG signals have low values (skin shapes are not visually appreciated) and, consequently, a decision about this pixel is hard based on this type of information. In these cases, the input related with hue is decisive and it is able to improve the output of the system up to provide an acceptable result in skin detection. Despite all, among these cases, there are situations, as happens in IV-M1, where PPG input can slightly improve the output that provide only the hue input, for example, helping in the detection of eyes. An example where both kind of input signals are good is II-M1.

- The influence of fuzzy logic in the system is relevant. It can be easily corroborated comparing the rows (e) and (f) of Fig. 6. In I-M1, I-F1 and V-M2, specially, fuzzy logic improves significantly results of crisp approach<sup>1</sup>.

<sup>1</sup>Unlike the fuzzy approach in which a element can be-

- The performance of this first rule-base is good since, in the figures of the row (f) it is already possible to distinguish visually the skin of the image, which, in a perfect detection, should be equal to the figures shown of the row (i). However, in cases such as I-F1 or I-M1, the necessity to establish a good threshold that changes dynamically with the video sequences, is appreciated. With that desired threshold value, the output of the system would be similar to the ideal output (See rows (g) and (i)).

The performance of the second rule-base (it provides the searched threshold) has been evaluated numerically, comparing the best and the calculated threshold value. In 13 of the 22 processed video sequence, the committed error was less than 0.1. Although in the majority of the rest of the sequences the long to several sets with different membership grade, in the crisp approach, each element can only belong to one set. In this work, the limit between sets has been established as the middle point of the parameters of the fuzzy set. The output of the system in this case is obtained using a decision-tree.

error is a bit larger (between 0.15 and 0.25), this error do not have too much influence on the output of the system (see (h) and (i) rows of Fig.6). There are only two cases, III-M1 and I-II-TP, where the error is relevant (around 0.45). In them, the difference between the desired and the real output is significant.

The last two rows of Fig.6 show the results of an simple example in which a global PPG signal has been obtained from each set of extracted connected skin pixels in the image. To achieve it, after the skin detection carried out with the proposed system, a connected component labeling (CCL) algorithm has been also applied to discriminate between the different subjects in the image, for example, in case of I-II-TP. Later, the global signal for each blob is calculated, choosing for each frequency value of the new signal, the most frequent value in that frequency among all the skin pixels belonging to that blob. Choosing the mode value, although the signal was not good in all the pixels of the skin, the detection will be right and, as a result of it, the shape of the obtained global PPG signals is very similar to the shape of a signal obtained in a pixel belonging to the forehead of each subject using (de Haan et al., 2013). Finally, a peak detection is made in that global signal, allowing to obtain automatically the pulse rate value of each person. Except in case I-M1, in which the highest found peak (in 40 Mhz) doesn't correspond to the actual pulse rate (in 72.5 MHz), the pulse rate value is correctly detected with the proposed system.

## 6.1 Comparison with Other Techniques

The original idea to use rPPG for performing a high level task like skin-detection was first shown in (Schmitz, 2010) and claimed in (US 8542877, 2010). Apart from the presented contribution, other work where this method is used has been published recently (Gibert et al., 2013). In it, the estimation of pixels belonging to skin from a presence/absence of heart rate index, which is calculated using the mean and the maximum spectral power of the PPG signal in each region of the image, is addressed. Later, a cleaning processing of false detections is carried out, removing ROIs that are not surrounding by others ROIs with a valid heart rate value and including ROIs in the neighborhood of well-detected ROIs whose difference of pulse rate value with the true value was less than 3 beats per minute. Although (Gibert et al., 2013) did not propose subsequent use for improving the PPG analysis, in our benchmarking of the proposed system, pulse rate detection has been also carried out with an implementation of the (Gibert et al., 2013) method, as it was done in the previous section with

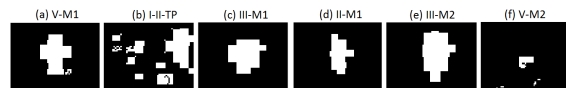


Figure 7: Skin detection achieved by the (Gibert et al., 2013) implementation.

the proposed system. The used implementation of the Fast ICA algorithm needed to obtain the PPG signal in that algorithm has been found in (Delorme's Web-Page). To get a fair comparison, the duration of the considered analysis window has been 60 sec. whereas the used ROI dimensions have been (12 x 12).

Fig. 7 shows the resulting skin detection. As it can be appreciated visually, comparing this figure with results in Fig. 6, the proposed system improves the attained resolution and definition of the pieces of skin in addition to increase the detection index (for example, in cases I-II-TP or V-M2). To support this visual impressions, Table 3, which gathers some quantitative measures of the quality of the skin extraction, has been also included. In addition to the true positive and negative rates (TPR and (1-FPR), respectively), this table shows values of other two overall measures, similarity and F-Measure, to also prove the improvement of the proposed system. As a result of this bad skin extraction with some sequences, the pulse rate detection is not so good. In some cases, such as I-II-TP, there is no peak for making the pulse rate detection, whereas in some other cases, e.g. V-M1 and V-M2, an incorrect peak is being detected.

## 7 CONCLUSIONS

The main contribution of our paper is a low-cost system for increasing the robustness of an earlier proposed pulse rate detector based on remote photoplethysmography. The system combines, by means of fuzzy logic, PPG and hue features in a video sequence

Table 3: Quantitative quality measures of the skin extraction. TN/TP = True negative/positive classified pixels, FN/FP = False negative/positive classified pixels.

		TPR	1-FPR	Similarity	F-Measure
		$\frac{TP}{TP+FN}$	$\frac{TN}{TN+FP}$	$\frac{TP}{TP+FN+FP}$	$\frac{2TP}{2TP+FN+FP}$
(Gibert et al., 2013)	V-M1	0.9422	0.8786	0.4988	0.6656
	I-II-TP	0.5678	0.7912	0.3072	0.4701
	III-M1	0.7734	0.9101	0.5879	0.7405
	II-M1	0.8947	0.9363	0.5936	0.7450
	III-M2	0.8707	0.9259	0.7020	0.8249
	V-M2	0.1779	0.9949	0.1730	0.2950
Proposed algorithm	V-M1	0.9911	0.9568	0.7534	0.8593
	I-II-TP	0.6773	0.9846	0.6384	0.7793
	III-M1	0.8771	0.9623	0.7745	0.8729
	II-M1	0.9904	0.9495	0.7065	0.8280
	III-M2	0.9682	0.9574	0.8506	0.9193
	V-M2	0.8470	0.9730	0.7346	0.8470

to arrive at a robust skin detection. Once the region-of-interest has been extracted, the already done PPG analysis is filtered and modified to make the pulse rate detection more confident. Achieved results on skin and pulse rate detection have been evaluated and benchmarked with a recent publication on this topic.

## ACKNOWLEDGEMENTS

The authors like to thank the colleagues from the Electronic Systems group, Dept. EE, of the Eindhoven University of Technology for acting as subjects in our test, and particularly S.D. Fernando and W. Wang for further assisting with the equipment and the recording, and Cosmin Sabarnescu for the code for estimating PPG signals that he build during his internship in the group.

This work was partially supported by TEC2011-24319 from the Spanish Government and P08-TIC-03674 from the Andalusian Regional Government (both with support from FEDER). E. Calvo-Gallego is funded by a FPU fellowship from the Spanish Government.

## REFERENCES

- Hertzman, A. B. (1937) *Photoelectric plethysmography of the fingers and toes in man*, Exp. Biol. Med., vol. 37, no. 3, pp. 529-534, 1937
- Allen, J. (2007), *Photoplethysmography and its application in clinical physiological measurement*, Physiological Measurement, vol. 28, no. 3, pp. R1R39
- Huelsbusch, M. and Blazek, V. (2002). *Contactless mapping of rhythmical phenomena in tissue perfusion using PPGI*, Proc. SPIE, vol. 4683, pp. 110-117
- Takano, C. and Ohta, Y. (2007), *Heart rate measurement based on a time-lapse image*, Med. Eng. Phys., vol. 29, pp. 853-857
- Verkruysse, W. and Svaasand, L.O. and Nelson, J.S. (2008), *Remote plethysmographic imaging using ambient light*, Opt. Exp., vol. 16, no. 26, pp. 21434/5
- Glass, K.A., Frishkoff, G.A., Frank, R.M. Davey, C. Dien, J. Malony, A.D. and Tucker, D.M. (2004), *A framework for evaluating ICA methods of artefact removal from multichannel EEG*, Proc. 5th Int. Conf. ICA 2004, Spain, Sept.
- Hülsbusch, M. (2008), *An image-based functional method for opto-electronic detection of skin-perfusion*, PhD Thesis, RWTH Aachen, Depart. of EE, (in German)
- Lewandowska, M. and Ruminski, J. and Kocejko, T. and Nowak, J. (2011), *Measuring pulse rate with a webcam - A non-contact method for evaluating cardiac activity*, Proc. Federated Conf. Comput. Sci. Inform. Syst., pp. 405-410
- Poh, M.Z. and McDuff, D.J. and Picard, R.W. (2010), *Non-contact, automated cardiac pulse measurements using video imaging and blind source separation*, Optics Express, vol. 18, no. 10, pp. 10762-10774
- De Haan, G. and Jeanne, V. (2013), *Robust Pulse Rate From Chrominance-Based rPPG* IEEE Transactions on Biomedical Engineering, vol. 60, no. 10, pp. 2878/86
- Lempe, G. and Zaunseder, S. and Wirthgen, T. and Zipser, S. and Malberg, H. (2013), *ROI Selection for Remote Photoplethysmography* Bildverarbeitung für die Medizin, Springer Berlin Heidelberg
- De Haan, G. and Biezen, P.W. (1994), *Sub-pixel motion estimation with 3-D recursive search block-matching*. Signal Processing: Image Communication, vol. 6, n. 3
- De Haan, G. (2010), *Chapter 10: Motion compensation*. Digital Video Post Processing, Eindhoven, pp. 225/27
- Kelly, W. and Donnellan, A. and Molloy, D. (2008), *Screening for Objectionable Images: A Review of Skin Detection Techniques* IEEE International Machine Vision and Image Processing Conference
- Vezhnevets, V. and Sazonov, V. and Andreeva, A. (2003), *A survey on pixel-based skin color detection techniques*. Proc. Graphicon, vol. 3, pp. 8592
- Kakumanu, P. and Makrogiannis, S. and Bourbakis, N. (2007), *A survey of skin-color modeling and detection methods*. Pattern Recognition, vol. 40, no. 3
- Xfuzzy [Online] <http://www2.imse-cnm.csic.es/Xfuzzy/>
- Oberti, F. and Teschioni, A. and Regazzoni, C.S. (1999), *ROC curves for performance evaluation of video sequences processing systems for surveillance applications*. Proceedings International Conference on Image Processing, ICIP, vol. 2, pp. 949-953
- Schmitz, G.L.L.H. (2010) *Video camera based photoplethysmography using ambient light* Master graduation paper, Electrical Engineering, Publ. of TUE
- Jeanne, V. and De Bruijn, F.J. and Vlutters, R. and Cennini, G. and Chestakov, D (2010) *Processing images of at least one living being* US Patent 8,542,877
- Gibert, G. and DAlessandro, D. and Lance, F. (2013), *Face detection method based on photoplethysmography*. 10th IEEE International Conference on Advanced Video and Signal Based Surveillance (AVSS)
- Delorme's WebPage [Online], <http://scnc.ucsd.edu/arno/>